Journal of Radioanalytical Chemistry, Vol. 43 (1978) 489–521

A NEW METHOD OF QUENCH MONITORING IN LIQUID SCINTILLATION COUNTING: THE H NUMBER CONCEPT*

D. L. HORROCKS

Scientific Instruments Division, Beckman Instruments, Inc., Irvine, California 92713 (USA)

(Received August 8, 1977)

The quench level of different liquid scintillation counting samples is measured by comparison of the responses (pulse heights) produced by the same energy electrons in each sample. The electrons utilized in the measurements are those of the maximum energy (E_{max}) which are produced by the single Compton scattering process for the same energy gamma-rays in each sample. The relation of the E_{max} response produced in any sample is related to the E_{max} response produced in an unquenched, sealed standard. The relation, difference in response on a logarithm response scale, is defined as the "H Number," H#. The H# is related to the counting efficiency of the desired radionuclide by measurement of a set of standards of known amounts of the radionuclide and different amounts of quench (standard quench curve). This report presents the theory of the H# concept. Several of the unique features of the H# method are discussed. Quench curves based upon the H# are compared to other previously used methods of quench monitoring.

Introduction

The liquid scintillation system is what is commonly called a "proportional response" system. The response produced (pulse height) is proportional to the energy, from the radionuclide transformation, that is absorbed by the liquid scintillation system. For electron excitation, it has been demonstrated that the response is directly proportional to the electron energy or, at least, to the amount of the electron energy which is dissipated in the liquid scintillation media.[1]

The loss of kinetic energy of the electron (beta particle, conversion electron, Compton electron etc.) produces excited molecules in the liquid scintillation medium through direction excitations, ionization followed by ion recombination, secondary electrons, and other processes. The excited molecules created in this primary interaction are excited solvent molecules. Excited solvent molecules are not good scintillators. Therefore, small amounts (3–5% by weight) of very efficient fluorescers (solutes) are added. At the proper concentration of these solutes, the excitation

*D. L. Horrocks, US Patent No. 4,075,480.

energy migrates and transfers, essentially quantitatively, from the solvent molecules to the solute molecules producing excited solute molecules. These excited solute molecules then emit photons (one photon per each excited molecule). The number of photons emitted is proportional to the energy of the electron which was stopped within the medium.

The photons are transmitted through the scintillation medium escaping through the walls of the sample container (bottle or vial). From this point on, the light detectors (multiplier phototubes and light guide optics) and electronic system determine the response produced. The photons are collected by a special light collection system onto the face of two multiplier phototubes. The photocathode of the multiplier phototube absorbs a fraction of the photons (quantum efficiency) using that absorbed energy to release electrons from the inside surface of the photocathode. The number of electrons is proportional to the number of photons which strike the face of the multiplier phototube. These electrons, called photoelectrons, are accelerated and focused onto a dynode material which has the property of producing an average of 4 electrons for each electron which strikes the dynode. These 4 electrons are then accelerated to a second dynode, and again, each electron releases 4 electrons giving a total of 16 electrons leaving the second dynode. This process continues through the total number of dynodes of the multiplier phototube. For a 10 dynode tube, the total gain would be: Gain $= 4^{10} = 1.05 \cdot 10^6$ or a total of one million electrons are created for each electron emitted from the photocathode.

A constant fraction of the electrons from a single event are collected on the anode of the multiplier phototube, and an electronic circuit integrates the current producing a voltage pulse which is proportional to the total number of electrons produced by the single event.

The voltage pulses from each multiplier phototube of the pair are used to distinguish between real events and random noise. The coincidence circuit will produce a gating pulse for every time that pulses are produced in each multiplier phototube within the resolving time of the system ($15–20 \cdot 10^{-9}$ sec). The voltage pulses from the two multiplier phototubes are also summed to give a truer pulse height representation of the event and to provide a better signal-to-noise ratio.

In commercially available liquid scintillation systems, most factors which determine the measured response for any event are constant. The only variable factor is the response created in the sample itself. Each sample can have varying numbers of photons for equal energy input because of different amounts of "quench". Quenching is defined as any process which reduces the number of photons observed for a given amount of energy input to the liquid scintillation solution. The two main types of quenching are:

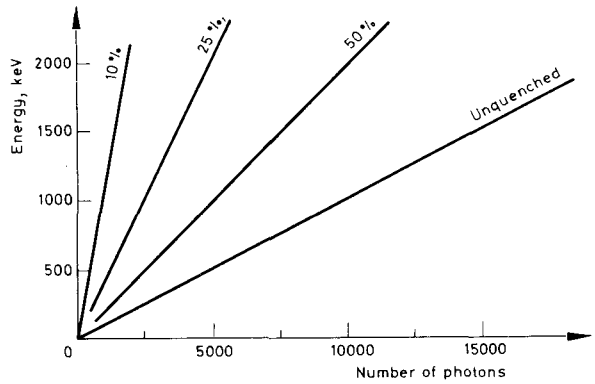

Fig. 1. Relative quench effect on the photon yield for different electron energies

Table 1
Relative photon yields as function of electron energy
for different amounts of quench

Electron energy, keV	Relative number of photons produced when sample quench level is			
	Unquenched	50%	25%	10%
1	10	5	2.5	1
18	180	90	45	18
156	1 560	780	390	156
500	5 000	2 500	1 250	500
1 000	10 000	5 000	2 500	1 000
1 710	17 100	8 550	4 275	1 710

(a) Impurity – which reduces the number of photons produced.

(b) Color – which reduces the number of photons through optical absorption of a fraction of the photons produced. The effect of color quenching is dependent upon the pathlength and the optical density and concentration of the absorbing material.

Within a given liquid scintillation sample, the quenching process(es) are proportional – i.e., if any energy event has a 50% reduction in photon yield, every energy event will have a 50% reduction in photon yield. If all other factors are constant (i.e., MPT gain, electronic amplification, etc.), then the measured response will be reduced by the same fraction. Fig. 1 shows the response vs. energy relationships for liquid scintillation samples with different amounts of quench relative to an unquenched sample. The same data are shown in Table 1.

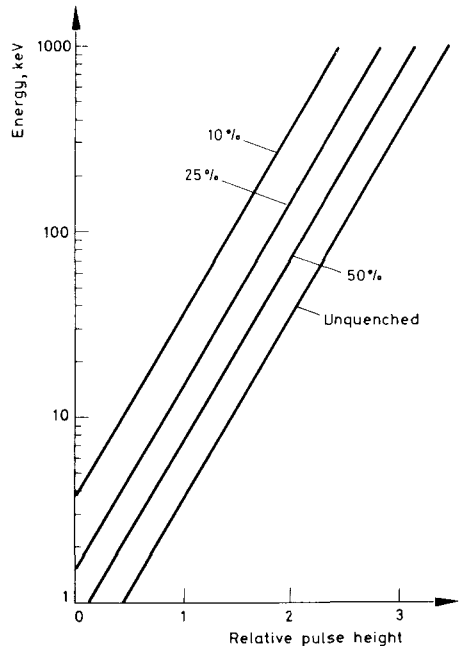

Fig. 2. Relative quench effect on the relative logarithmic response for different electron energies

Some commercial liquid scintillation systems (i.e., the Beckman LS-8000 Series) utilize the logarithmic response relationship. In these systems, the pulse height response is converted into a new pulse height response equal to the logarithm of the initial pulse height. This conversion makes it possible to handle pulses that initially differ by a factor of 1000 to 1 in pulse height with a single amplifier and pulse height analyzer.

The effect of quench on the measured pulse height response relationships for a logarithmic system are listed in Table 2, and shown graphically in Fig. 2. It will be noted that a 50% reduction of photon yield due to quenching leads to a constant difference of 0.30103 (the logarithm of 2) between the relative logarithmic response relationships.

Theory

Compton scattering

For some time it has been common practice to utilize a gamma emitting radionuclide external to the sample to measure the response of liquid scintillation-sample mixtures. The response can be calibrated through the use of a set of samples con-

Table 2
Relative logarithmic response as a function of electron energy at different quench levels

Electron energy, keV	Relative logarithm response when sample quench level is			
	Unquenched	50%	25%	10%
1	0.447	0.146	−0.155	−0.553
18	1.702	1.401	1.100	0.702
156	2.640	2.339	2.038	1.640
500	3.146	2.845	2.544	2.146
1 000	3.447	3.146	2.845	2.447
1 710	3.680	3.379	3.078	2.680
Difference		0.30103	0.30103	0.39794

taining a known amount of a given radionuclide but with different levels of quench. The "quench curve" is a plot of the counting efficiency of the sample containing radionuclide vs. the response produced by the external gamma-ray radionuclide on that same sample. Samples with unknown amounts of this radionuclide are then calibrated by measuring the response produced by the external gamma-ray radionuclide and calculating the counting efficiency from the quench curve. In this manner, all samples, regardless of their quench level, are corrected to a common quench level for comparison of relative amounts of the radionuclide in different samples.

Gamma-rays interact with matter in one of three ways: (1) pair production, (2) Compton scattering, or (3) photoelectric effect. Fig. 3 shows the relationship between the relative probability of these three types of interactions as a function of the energy of the gamma-rays. The process of pair production has an energy threshold of 1.02 MeV (twice the energy equivalent of the rest mass of an electron). Any gamma-ray of energy less than 1.02 MeV cannot interact with matter by the process of pair production. At the other end of the energy scale, the photoelectric effect is predominant only at gamma-ray energies below 20 keV. Compton scattering is the predominant mode of interaction for gamma-ray with energies between 20 keV and 10 MeV. Thus by choice of the gamma-emitting radionuclide with gamma-ray energies between 0.1 and 3.0 MeV, the Compton scattering process will be the prominent mode of interactions of the gamma-rays with the interacting media (in this case, the liquid scintillation solution).

The Compton scattering process is independent of the scattering media. The gamma-rays collide with essentially free electrons in the media each imparting a

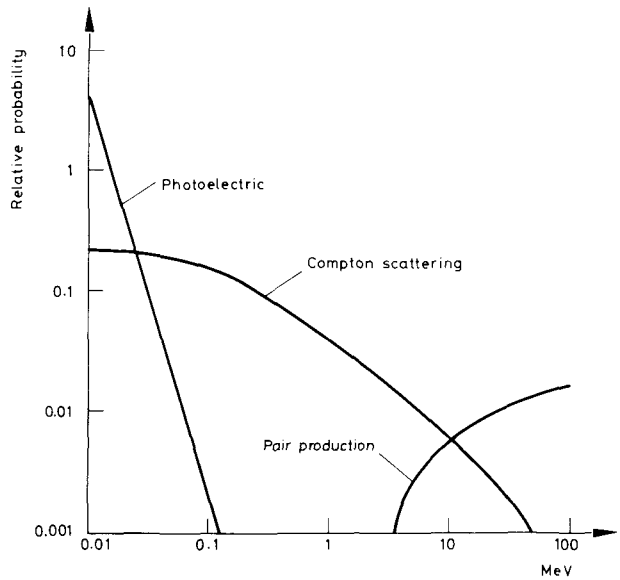

Fig. 3. Relative probabilities of pair production, Compton scattering, and photoelectric effect as a function of gamma-ray energy

part of its kinetic energy to the electron which results in a scattered gamma-ray of energy less than the initial gamma-ray energy, E_{γ_0}. Total energy (and momentum) is conserved;

$$E_{\gamma_0} = E_e + E_{\gamma_1} \tag{1}$$

where E_e – energy of the scattered electron;
E_{γ_1} – energy of the scattered gamma-ray.

The Compton scattering process is shown diagrammatically in Fig. 4.

The division of the energy E_{γ_0} between E_e and E_{γ_1} is only a function of the angle at which the gamma-ray collides with the electron. The number of scattering events is a function of the gamma-ray flux and the number of electrons (electron density) in the scattering medium.

Because of their difference in mass (essentially zero for the gamma-ray and $5.486 \cdot 10^{-4}$ AMU for the electron) the gamma-ray will never impart its total energy to the electron. A maximum amount of energy, E_{max}, will be transferred to the electron for a direct head-on collision with the gamma-ray scattered at 180°

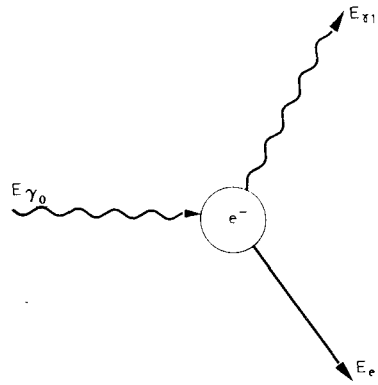

Fig. 4. Diagram of the Compton scattering process for gamma-ray of energy $E_{\gamma o}$

and retaining the residual amount of the energy ($E_{\gamma_0} - E_{max}$). The value of E_{max} is given by the expression;

$$E_{max} = \frac{(2\,E_{\gamma_0})^2}{2\,E_{\gamma_0} + 0.51} \qquad (2)$$

where energies are expressed in MeV and 0.51 MeV is the energy equivalent of the electron at rest. It is evident, from Eq. (2), that the value of E_{max} is only dependent upon the energy of the gamma-ray, E_{γ_0}. Table 3 lists the values of E_{max} for several E_{γ_0} values.

The probability of any value of E_e is equal up to the value of E_{max}. Thus a theoretical plot of the number of scattered electrons of given energy vs. the energy of the scattered electron would be represented by Fig. 5. There will be no electrons

Table 3
Values of E_{max} for different gamma-ray energies, E_{γ_0}

E_{γ_0}	E_{max}
0.356	0.207
0.510	0.340
0.662	0.478
1.280	1.067
2.750	2.517

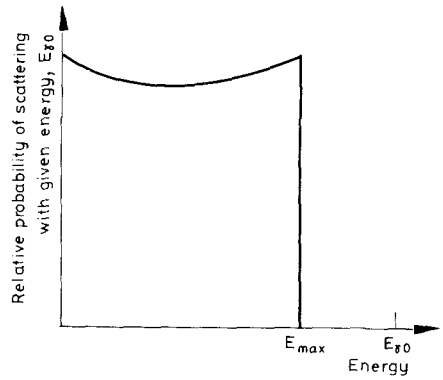

Fig. 5. The number of Compton scattered electrons of given energy for gamma-ray of energy $E_{\gamma 0}$

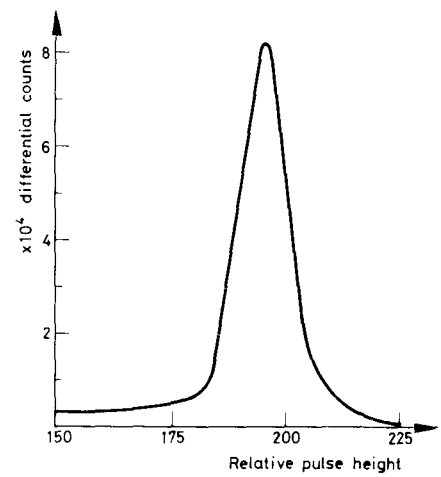

Fig. 6. Pulse height distributions for 0.369 MeV electrons from ^{113m}In in a liquid scintillation system

of energy greater than E_{max}. (This fact is predicated in the assumption that only a single Compton scattering per gamma-ray will occur.)

Pulse height response

The measured distribution of Compton scattered electrons will be different than the theoretical distribution because no detection system is theoretically perfect. Any detection system (including a liquid scintillation system) will produce a spread of responses for the same energy event which is detected by that system. Fig. 6

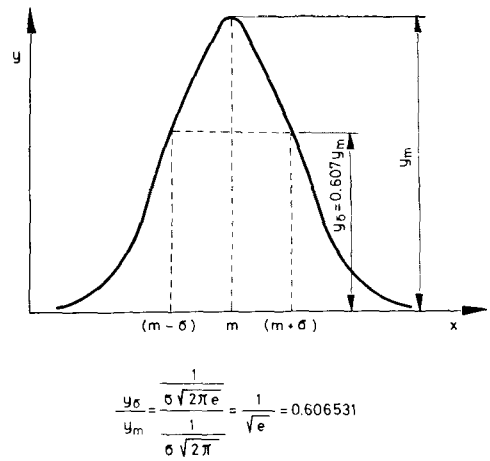

Fig. 7. Gaussian distribution plot of y vs. x showing the relationships for the values of σ, y_m and y

shows the distribution of pulses from a liquid scintillation solution for detection of essentially monoenergetic electrons. Electrons of 0.369 MeV energy from ^{113m}In are measured for a source of ^{113}Sn – ^{113m}In (as an organic complex) dissolved in a liquid scintillation solution. The pulse height spectrum was obtained on a Beckman Liquid Scintillation System with logarithmic response (i.e., the linear pulse height response is converted to a pulse height proportional to the logarithm of the linear pulse height response).

Since the spread of pulse height responses is statistically random, the distribution can be described by the equation for a Gaussian distribution;

$$y = \frac{1}{\sigma\sqrt{2\pi}} \, e^{-(x-m)^2/2\sigma^2} \tag{3}$$

where the terms of the equation are illustrated in Fig. 7;

From Eq. (3) several relationships can be derived. First it is necessary to define the term σ (sigma) of a Gaussian distribution. The term σ is defined as the variance of the Gaussian distribution and 0.6827 of all the total area of the Gaussian distribution will fall between values of x equal to $(m - \sigma)$ and $(m + \sigma)$. (In measurement of radioactivity rates, σ is referred to as the standard error.) At the values of x equal to $(m \pm \sigma)$ a Gaussian distribution has some unique properties which are not

repeated at any other x values. The first derivative (or slope) of the equation gives a maximum value at x equal to $(m \pm \sigma)$;

$$\frac{dy}{dx} = \frac{-2(x-m)/2\sigma^2}{\sigma\sqrt{2\pi}} e^{-(x-m)^2/2\sigma^2} \tag{4}$$

Substituting $x = (m \pm \sigma)$ gives

$$\frac{dy}{dx} = \pm \frac{1}{\sigma^2\sqrt{2\pi e}} \text{ (a maximum)} \tag{5}$$

Substitution of any other value if x will give a value of dy/dx less than this.

Further, the second derivative (slope of the slope) gives a value of zero at the values of x equal to $(m \pm \sigma)$:

$$\frac{d^2y}{dx^2} = \left[\frac{-2(x-m)/2\sigma^2}{\sigma\sqrt{2\pi}}\right]\left[\frac{-2(x-m)}{2\sigma^2} e^{-(x-m)^2/2\sigma^2}\right] +$$

$$+ \left[\frac{-2/2\sigma^2}{\sigma\sqrt{2\pi}}\right]\left[e^{-(x-m)^2/2\sigma^2}\right] \tag{6}$$

Substituting $x = (m + \sigma)$ gives

$$\frac{d^2y}{dx^2} = \left[\frac{-2\sigma/2\sigma^2}{\sigma\sqrt{2\pi}}\right]\left[\frac{-2}{2\sigma^2} e^{-1/2}\right] + \left[\frac{-2/2\sigma^2}{\sigma\sqrt{2\pi}}\right] e^{-1/2} =$$

$$= \left[\frac{1}{\sigma^3\sqrt{2\pi}} - \frac{1}{\sigma^3\sqrt{2\pi}}\right] e^{-1/2} = 0 \tag{7}$$

Similarily, $d^2y/dx^2 = 0$ upon substituting $x = (m - \sigma)$.

And finally the value of y at x equal to m is:

$$y_m = \frac{1}{\sigma\sqrt{2\pi}}. \tag{8}$$

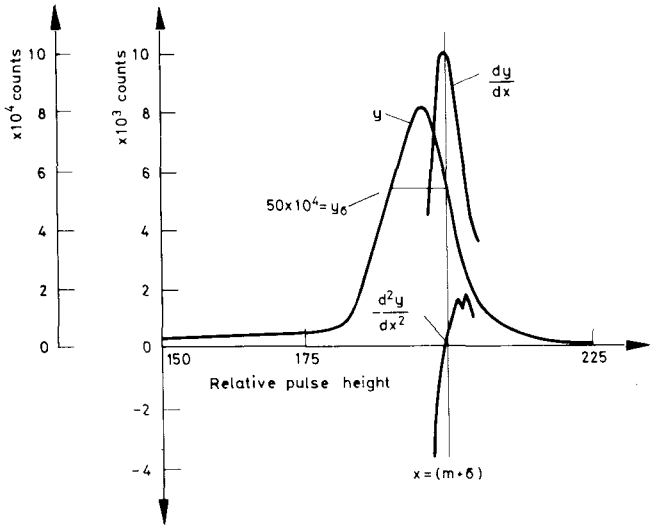

Fig. 8. Pulse height distribution for 0.369 MeV electrons along with dy/dx and d^2y/dx^2 plots and evaluation of y

The value of y at x equal to $(m \pm \sigma)$ is:

$$y_\sigma = \frac{1}{\sigma \sqrt{2\pi}} e^{-1/2} \tag{9}$$

The ratio of y_σ/y_m will be equal to:

$$\frac{y_\sigma}{y_m} = \frac{\frac{1}{\sigma \sqrt{2\pi}} e^{-1/2}}{\frac{1}{\sigma \sqrt{2\pi}}} = 0.606531 . \tag{10}$$

Thus for any Gaussian distribution, the value of y for which d^2y/dx^2 is equal to zero is y_σ or;

$$y_\sigma = 0.606531\ y_m . \tag{11}$$

The distribution plotted in Fig. 6 is replotted in Fig. 8 along with plots of dy/dx and d^2y/dx^2. It will be noted that dy/dx gives a maximum value at x equal to

Table 4
Evaluation of value of x equal to $(m + \sigma)$ for plots in Fig. 8

For criteria	Value of x
dy/dx = maximum	~200
$d^2y/dx^2 = 0$	200.25
$Y_\sigma = 0.607\ y_m$	200.74

about 200. The value of d^2y/dx^2 is equal to zero at a value of x equal to 200.25. Using the relationship

$$y_\sigma = 0.607\ y_m$$

and the value of y_m equal to $8.24 \cdot 10^4$, the value of y_σ is calculated to be $5.00 \cdot 10^4$. The value of x for $y = 5.00 \cdot 10^4$ is 200.74. Table 4 summarizes the values of x for which each of the criteria for a Gaussian distribution is evaluated at x equal to $(m + \sigma)$. It can be seen that all values of x are within experimental error the same. Thus the distribution obtained for measurement of essentially monoenergetic electrons in a liquid scintillation system can be fit to the equation for a Gaussian distribution.

Fig. 9 shows the distribution of pulses obtained for the Compton scattered electrons produced in a liquid scintillation solution by the gamma-rays (0.662 MeV) from a $^{137}Cs - ^{137m}Ba$ source. (The only gamma-rays which escape the source holder are the 0.662 MeV gamma-rays. The 32 keV Ba X-rays are totally absorbed in the source tube holder.) The use of a radionuclide which gives a single gamma-ray energy will give a single Compton distribution while a radionuclide with two or more gamma-ray energies will produce two or more Compton scattered electron distributions with an E_{max} for each gamma-ray energy. Fig. 10 shows the distributions obtained with a single energy gamma-ray source ($^{137}Cs - ^{137m}Ba$) and a source of gamma-rays of two different energies (^{22}Na). Table 5 summarizes the expected values of E_{max} for these radio-nuclides.

Since each different energy gamma-ray produces its own distribution of Compton scattered electrons from zero energy to E_{max}, the spectrum for ^{22}Na shows one distribution superimposed upon another. In order to utilize the Compton distribution for quench monitoring it is best to have a single energy gamma-ray source which will present no interferring Compton distributions. It is also desirable to have the gamma-ray energy sufficiently high enough to provide a wide dynamic range of quench monitoring but not too high an energy as to require a very large

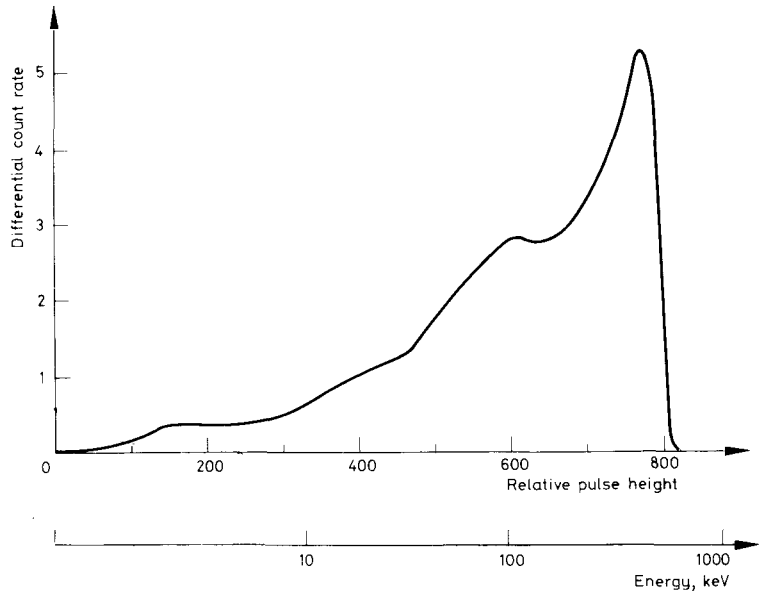

Fig. 9. Pulse height distribution for Compton scattered electrons produced by the 0.662 MeV gamma-rays from $^{137}Cs - {}^{137}Ba$ interaction with a liquid scintillation solution

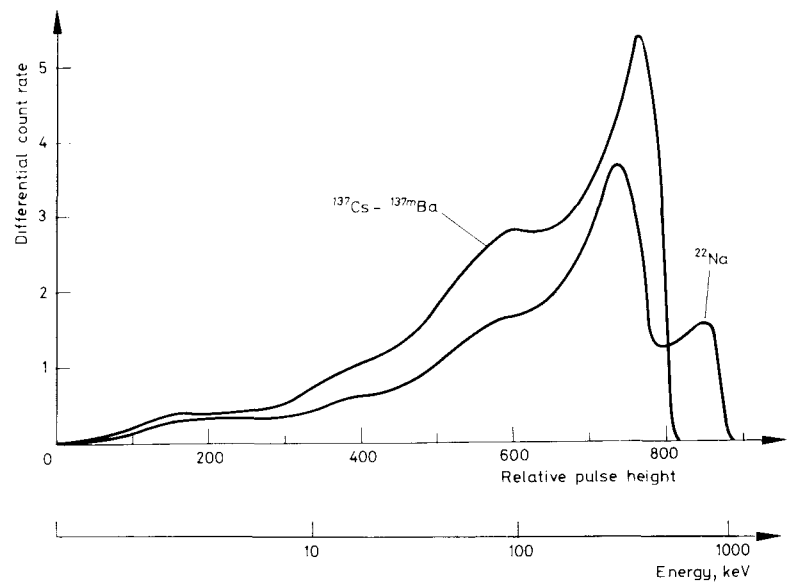

Fig. 10. Pulse height distributions for Compton scattered electrons produced in a liquid scintillation solution by gamma-rays from $^{137}Cs - {}^{137m}Ba$ (0.662 MeV) and ^{22}Na (0.51 MeV and 1.28 MeV)

Table 5
Gamma-ray energies, E_{γ_0}, and E_{max} values for two radionuclides, $^{137}Cs-^{137m}Ba$ and ^{22}Na

Radionuclide	E_{γ_0}, MeV	E_{max}, MeV
$^{137}Cs-^{137m}Ba$	0.662	0.478
^{22}Na	0.510	0.340
	1.280	1.067

Table 6
List of some desirable properties of $^{137}Cs-^{137m}Ba$ radionuclides for use as a source for this new method of quench monitoring

Desirable Property	Property of $^{137}Cs-^{137m}Ba$
Single energy	0.662 MeV*
E_{max} sufficiently high to provide dynamic range	0.478 MeV
Long half-life	30 y
Moderate Compton scattering yield	40 μCi source yields about 10^6 Compton scattered electrons per minute with Beckman LS-8000 geometry and 16–18 ml of liquid scintillation solution.

*The 32 keV Ba K X-rays are not detected as they are not energetic enough to penetrate the mounting for the gamma-ray source.

amount of the radionuclide in order to have a sufficient number of Compton scattered electrons produced (per unit time) in the finite volume of the liquid scintillation solution. Fig. 3 shows the relative probability of Compton scattering as a function of gamma-ray energy. It is also desirable to have a source which will not decay too rapidly. One radionuclide which seens to satisfy these criteria is $^{137}Cs-^{137m}Ba$. Subsequent discussions will deal with the use of $^{137}Cs - ^{137m}Ba$ but any radionuclide which satisfies these criteria could also be used. Table 6 summarizes some of the properties of $^{137}Cs - ^{137m}Ba$.

If this method is to be viable, it is necessary that the pulse height distribution for a monoenergetic electron excitation give a Gaussian distribution at different quench levels. Fig. 11 shows pulse height spectra for 369 keV electrons from ^{113m}In in a liquid scintillation solution at different quench levels. As predicted by the Gaussian theory, the value of y_m decreases with decreased pulse height value of x_m and the

Table 7
Pulse height values for which each of these Gaussian criteria are satisfied at four different quench levels

Relative quench level	Energy equivalent*	Pulse height for which		$d^2y/dx^2 = 0$
		$y_\sigma = 0.607\ y_m$	dy/dx = max.	
1.00	369	200.74	200	200.25
1.89	195	180.54	181	180.37
9.60	38.4	129.22	130	129.51
50.20	7.4	76.60	76	75.10

*Electron energy which would produce the same pulse height response in a sample with relative quench level of 1.00.

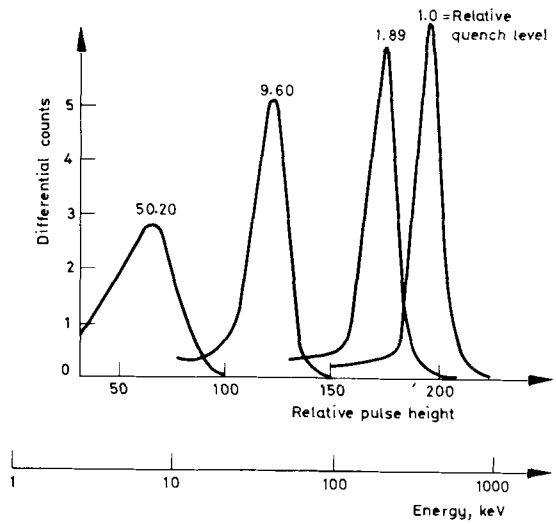

Fig. 11. Pulse height distributions for 0.369 MeV electrons in a liquid scintillation solution with different amounts of a quenching agent

distribution becomes broader (i.e., σ becomes larger). Also, the higher pulse height side of the distribution satisfies all the criteria of the Gaussian equation. Table 7 summarizes the values of pulse height for which x is equal to $(m + \sigma)$ for each quench level. The most quenched sample exhibited a greater than 50 decrease in light yield. The fact that all three values of pulse height, at a given quench level, according to different criteria are nearly the same prove that the Gaussian distribution is valid over a very wide dynamic quench range.

Table 8
Evaluation of pulse height which evaluates the Gaussian parameters for the scintillation solution shown in Fig. 12

Value of pulse height for which		
$y_\sigma = 0.607\ y_m$	dy/dx = maximum	$d^2y/dx^2 = 0$
169.3	169.5	169.6

Actual count data			
Pulse height	Counts	Δ[a]	Δ^2 [b]
172	976	134	
171	1110		42
170	1286	176	116
169	1578	292	−176
168	1694	116	−87
167	1723	29	

$y_m = 2440$
$y_\sigma = 0.607\ y_m = 1481$

[a] $\Delta = n_n - n_{n-1}$.
[b] $\Delta^2 = \Delta_n - \Delta_{n-1}$.

Compton edge measurement

These same criteria can be used in evaluating the pulse height distribution for Compton scattered electrons of energy E_{max}. The electrons of energy E_{max} are monoenergetic and there are no electrons of energy greater than E_{max}. Thus the upper edge of the Compton distribution can be considered as the upper half of a Gaussian distribution for electrons of energy E_{max}. Actually, there are Compton electrons of energy just less than E_{max} which also will contribute to the pulse height distribution of the Compton edge. However, in practice the contributions from these electron energies do not render the shape of the Compton edge non Gaussian. There is still only *one* pulse height value for which the value of $d^2y/dx^2 = 0$. Fig. 9 shows the pulse height distribution for the Compton electrons produced by the 662 keV gamma-rays from a $^{137}Cs - {}^{137m}Ba$ source. Table 8 summarizes the actual count data and the pulse height values obtained by three methods of deter-

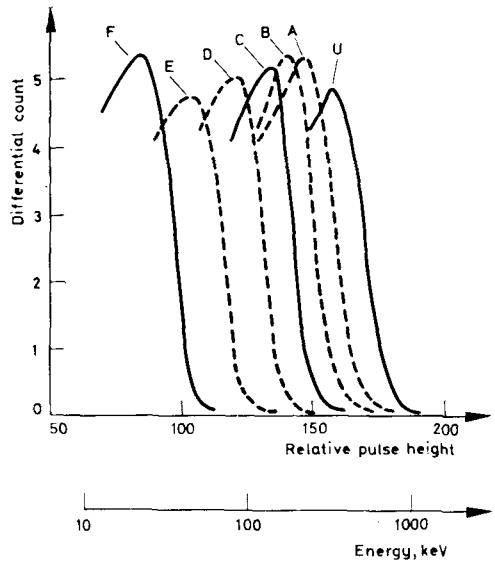

Fig. 12. Pulse height distributions of the upper edge of Compton electron distributions from scattering by 0.662 MeV gamma-rays in set of ^{3}H samples with different levels of quench

mining the inflection point of the Compton edge; (1) $y_\sigma = 0.607\, y_m$, (2) dy/dx = maximum and (3) $d^2y/dx^2 = 0$. Since all values are the same, it is evident that the Compton edge is indeed described by the Gaussian equation.

Fig. 12 shows the Compton edge spectra obtained for a series of ^{3}H quenched samples which were exposed to the gamma-rays from the $^{137}Cs - ^{137m}Ba$ source. These spectra (like those shown in the previous figures) were obtained using a multichannel analyzer as described previously.[2] Table 9 summarizes the data obtained with these samples.

H# definition

In a logarithmic energy-response relationship, the following equation;

$$PH = a + b \log E, \tag{12}$$

relates the measured pulse height (PH) on some arbitrary scale (discriminator divisions, channels, etc.) as a function of the excitation energy (E) in keV. "a" is the pulse height response for a 1 keV electron and "b" is the slope. For each level of quench there will be a different equation with the same value of "b" but different values of "a".

For an unquenched system (N_2 – saturated, flame sealed standards) the relationship could be represented by:

$$PH_o = a_o + b \log E \tag{13}$$

Table 9
Data for set of ^3H quenched samples relating counting efficiency, ESCR and pulse height of inflection point (from Gaussian parameters)

Sample	ESCR[a]	^3H counting efficiency, %	Pulse height of inflection point	Relative quench[b]	Energy equivalent,[c] keV
U	0.737	60.0	169.3	1.00	478.0
A	0.682	54.1	159.0	1.46	328.0
B	0.646	49.7	150.0	2.03	236.0
C	0.586	41.4	142.0	2.71	176.5
D	0.509	32.2	130.5	4.12	116.0
E	0.376	20.5	115.0	7.24	66.0
F	0.081	9.9	95.5	14.71	32.5

[a]External Standard Channels Ratio.
[b]The amount that the light output for the 478 keV Compton electrons has been reduced by the quench.
[c]The energy equivalent of an electron which would produce the same response in the unquenched liquid scintillator as the 478 keV electrons do in the quenched liquid scintillator.

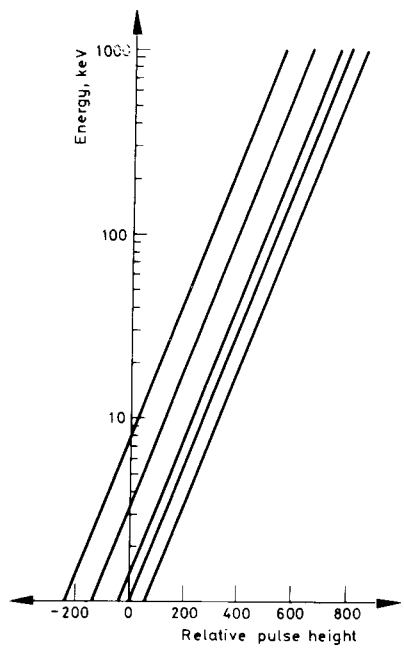

Fig. 13. Pulse height response vs. log of electron energy at different quench levels

Table 10
Relative pulse height response (log conversion) at different quench levels as measured by the H# value

Electron energy, keV	Pulse height response at				
	H# = 0	H# = 58	H# = 98	H# = 198	H# = 298
1	58	0	−40	−140	−240
10	328	270	230	130	30
100	598	540	500	400	300
1000	868	810	770	670	570

Likewise for any quenched sample the relationship will be given by;

$$PH_q = a_q + b \log E \tag{14}$$

The value of "a" will be different for different amounts of quench in the samples. The difference between the measured pulse height responses for a given energy will be;

$$PH_o - PH_q = a_o - a_q + b \log E - b \log E = a_o - a_q \tag{15}$$

This is the definition of the H# namely;

$$PH_o - PH_q = H\# \tag{16}$$

Upon substituion of the H# definition into Eq. (15), the following relationship is obtained;

$$a_q = a_o - H\# \tag{17}$$

The pulse height-energy relationship for any liquid scintillator sample (quenched or unquenched) thus becomes;

$$PH = a_o - H\# + b \log E \tag{18}$$

Considering a liquid scintillation system which has an arbitrary pulse height scale of 0–1000 divisions and values; a = 58, and b = 270.

The typical pulse height responses for electrons of energies of 1, 10, 100 and 1000 keV at selected quench levels, designated by H# values of 0, 58, 98, 198 and 298 are shown in Table 10 and Fig. 13. If any pulse which exceeded the zero

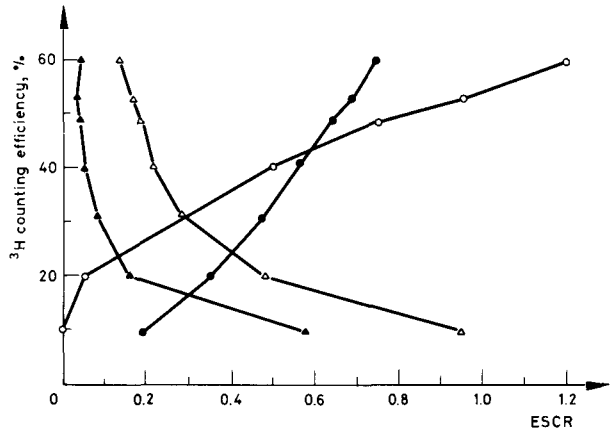

Fig. 14. Different plots of ESCR values vs. ^{3}H counting efficiency for the same samples but different choices of the window settings for the two counting channels for Compton generated pulses

threshold were counted, then the theoretical minimum detectable energy for the different quench levels would be as shown in Table 11. As quenching becomes greater, it requires more energy to produce enough photons to give a measurable response.

An advantage of the use of H# is evident by the fact that any sample can only have one H# value. This is different from other methods of quench monitoring

Table 11
Theoretical minimum detectable energy of electrons at different quench levels as measured by the H# value

H#	Theoretical minimum detectable energy, keV at zero pulse height. Based on Table 11 and Fig. 13
0	0.34
58	1.00
98	1.40
198	3.30
298	7.80
400	18.50

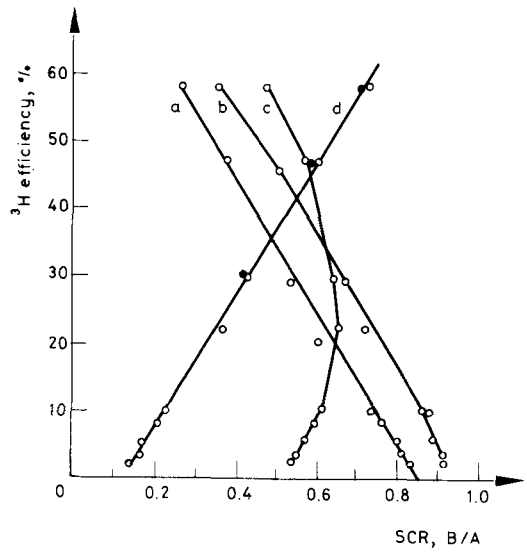

Fig. 15. Different plots of SCR values vs. ^{3}H counting efficiency for the same samples but different choices of the window settings for the two counting channels for ^{3}H generated pulses

such as sample channels ratio (SCR), external standard count rate (ESCPM) and external standard channels ratio (ESCR). These three methods can give essentially large and varied numbers of values of the quench measuring value, depending upon the choice of the settings for the counting channels used. Figs 14 and 15 show different quench curves for the same samples with different choices of counting channels for ESCR and SCR methods of quench monitoring.

Both SCR and ESCR methods have a limited range because, at some point, they become invariant with changing quench. Figs 16 and 17 show how a ratio can become constant at a given quench level and remain constant at all greater quench levels. The dynamic range of the H# method is only limited by the quench level at which the inflection point of the Compton edge is no longer measurable.

Since the H# is unique, it can be considered the universal quench parameter. Any properly calibrated system with H# capabilities should give, within statistical limits, the same H# value for equally quenched samples. Thus different laboratories now have a parameter which can be used to correlate experimental results. Also experiments done at different times can easily be compared through the H# values.

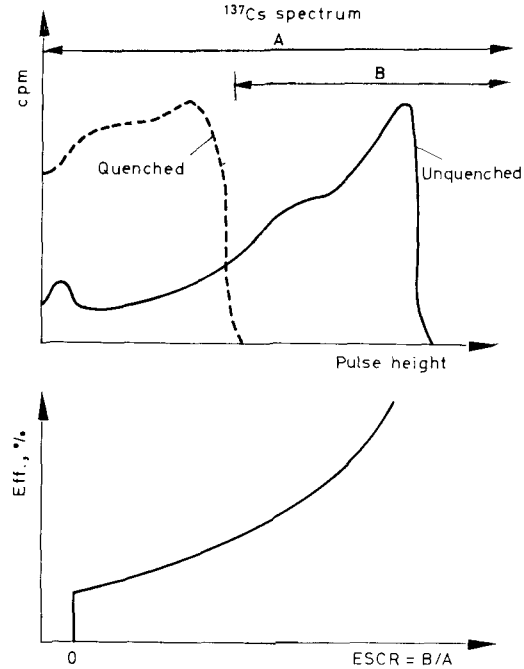

Fig. 16. Selection of window settings and count ratio as function of quench showing limiting range

Two instruments may not have the same counting efficiencies due to differences in multiplier phototubes, but the H# values should be the same, within statistical limits, at the same quench level.

Results

The following results were obtained using a commercially available liquid scintillation system which has the H# concept as an integral part of the system; the Beckman LS-8000 Liquid Scintillation System. Fig. 18 shows typical plots of H# versus counting efficiency for tritium and ^{14}C containing samples.

H# repeatability

The Beckman LS-8000 Series systems are designed to give H# repeatability such that the calculated counting efficiency based on the spread of H# values will statistically ($\pm 2\,\sigma$) be within ±1% efficiency of the average calculated counting efficiency.

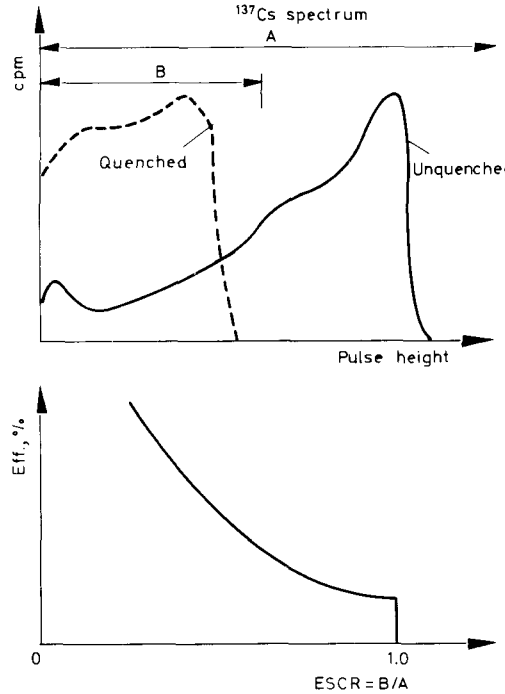

Fig. 17. Selection of window settings and count ratio as function of quench showing limiting range

This requires the comparison of the H# spread to a counting efficiency vs. H# plot for the particular radionuclide and quenching agent to be used in the experiment.

Fig. 19 shows the experimental data obtained for a quenched ^{3}H containing sample (18.68% counting efficiency). The sample was counted repeatedly (uniterrupted) over a period of 2.5 days with each H# determination followed by a 2 minute sample count. The 2 minute sample count is desirable to prevent fatigue of the multiplier phototube by continuous exposure to the gamma-ray source. Using the average H# value, the H# value plus 2 σ error value and the H# value minus 2 σ error value, the counting efficiencies based on the quench curve were calculated. The results are given in Table 12. The total spread of H# values is from 146 to 154. However, this distribution can be described as a normal distribution of values about some average value. The average value was calculated to be 151.4 and the $\pm 2\,\sigma$ error (95% confidence level) was calculated to be ± 2.5 H# units. This gives a range of 148.9 to 153.9 with a 95% confidence level. This means that only 5%

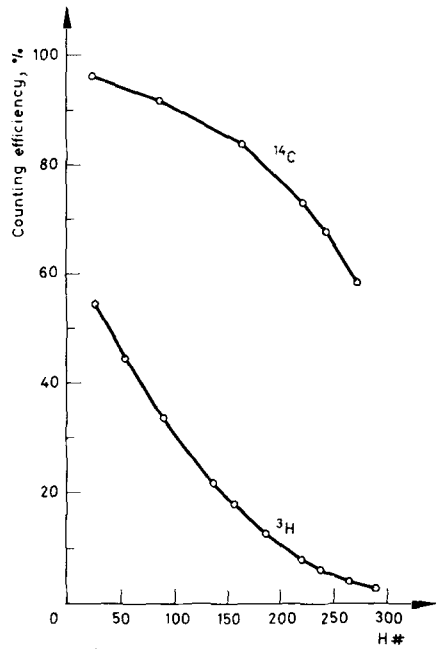

Fig. 18. Plots of counting efficiencies of ^{3}H and ^{14}C containing samples of different quench levels as a function of the H#

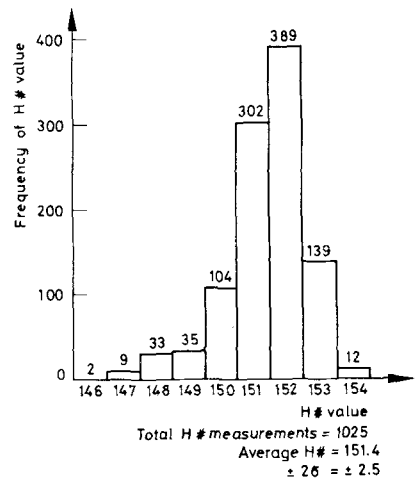

Fig. 19. Frequency pattern of H# values for single sample of moderate quench measured for 2.5 days

Table 12
Quench curve equation and calculated counting efficiencies for H# frequency plot of Fig. 19
Quench curve: Eff. (%) $= A + B\,(H\#) + C\,(H\#)^2 + D\,(H\#)^3$

$A = 65.894301$
$B = -0.455973$
$C = 0.001099$
$D = -0.00000097$

H# value	Counting Eff., %
Average $= 151.4$	18.68
Average $+2\sigma = 153.9$	18.21
Average $-2\sigma = 148.9$	19.17

Average Eff. $= (18.68^{+0.49}_{-0.47})$

Maximum = 154	18.18
Minimum = 146	19.73

(51) of the measured values should be outside this range. Indeed there were 44 values outside the range 149–154 although the distribution seems to be skewed to the low H# values.

The total 2 σ error spread of counting efficiency was less than ±0.5%. This is well below the quoted specification of ±1.0%. Even the total spread from lowest to highest measured H# values was only 1.55% counting efficiency.

Another sample of low quench (namely an air saturated, unquenched sample) was counted under the same conditions for 1.6 days. A total of 652 H# values were measured. The frequency of H# values are plotted in Fig. 20. Table 13 lists the calculated efficiencies and spread of efficiencies for the H# values measured. The ±2 σ error of the H# values produced only a ±0.39% counting efficiency error. The total spread of H# values (14–19) correspond to a change of 1.40% counting efficiency.

The H# value was measured for a single sample 100 times uninterrupted. After about 16 hours (overnight) the 100 measurements were repeated. Finally, after another 16 hours (overnight) the 100 measurements were repeated the third time. Fig. 21 shows the frequency distributions of the three experiments. The average H# values and calculated ±2 σ error values are in very good agreement.

In another experiment, each bottle of a series of quenched samples containing ^3H was measured 65 times. The samples were moved in the sample changing mechanism between each group of 10 measurements. Table 14 lists the data obtained

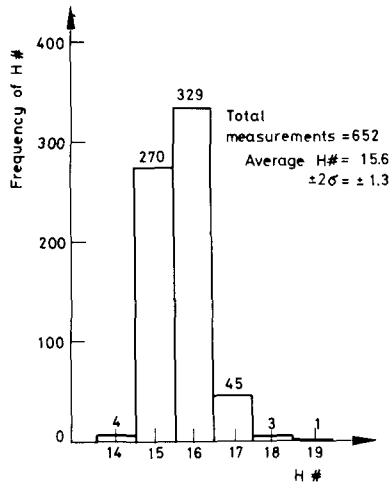

Fig. 20. Frequency pattern of H# values for single sample of low quench measured for 1.6 days

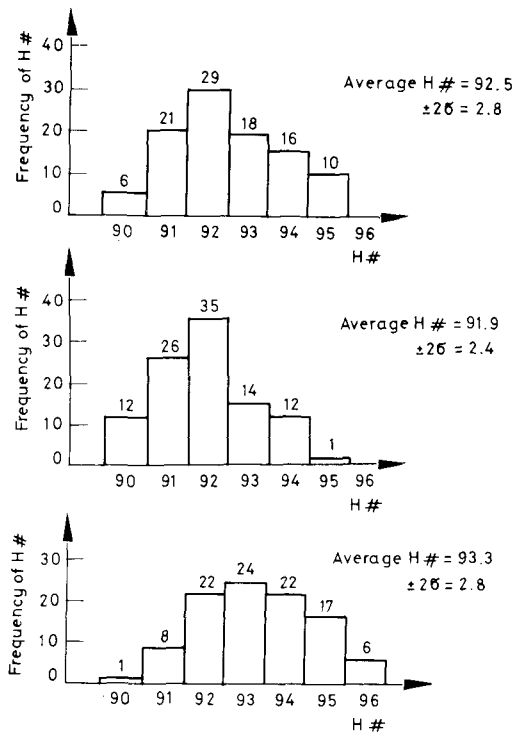

Fig. 21. Frequency patterns for H# values for a single sample measured for 100 times on each of 3 successive days

Table 13
Quench curve equation and calculated counting efficiencies for H# frequency plot of Fig. 20
Quench curve: Eff. (%) = A + B (H#) + C $(H\#)^2$ + D $(H\#)^3$

A = 60.720351
B = −0.289077
C = −0.000237
D = + 0.00000205

H# value	Counting Eff., (%)
Average = 15.6	56.15
Average $+2\sigma$ = 16.9	55.76
Average -2σ = 14.3	56.54

Average Eff. = (56.15 ± 0.39)%

Maximum = 19	55.23
Minimum = 14	56.63
Difference 5	1.40

Table 14
Calculated counting efficiencies for ^3H quench set based on frequency distribution of H# values

Number of measurements	Average H# $\pm 2\sigma$	Average counting eff., $\pm 2\sigma$ %
65	21.7 ± 2.8	$54.35^{+0.84}_{-0.82}$
65	31.5 ± 2.3	$51.43^{+0.70}_{-0.67}$
65	57.0 ± 2.8	$43.85^{+0.83}_{-0.83}$
65	84.5 ± 3.3	$35.84^{+0.95}_{-0.94}$
65	135.5 ± 4.0	$22.30^{+0.97}_{-0.95}$
65	194.5 ± 2.8	$10.60^{+0.43}_{-0.40}$
65	227.2 ± 3.1	$6.85^{+0.26}_{-0.23}$
65	268.4 ± 8.4	$5.70^{+0.32}_{-0.13}$

along with the 2 σ spread of H# values and counting efficiencies. In every case, the $\pm 2\,\sigma$ spread of H# values produced less than $\pm 1\%$ spread in calculated counting efficiencies.

Table 15
Values of the constants of cubic equation for best fit of H# vs. ^{3}H counting efficiencies plots obtained from 10 different sets of data

No.	A	B	C	D
1	67.315940	−0.460974	0.001027	−0.00000071
2	64.219007	−0.391243	0.000623	−0.00000001
3	65.952075	−0.443017	0.000962	−0.00000064
4	65.894301	−0.455973	0.001099	−0.00000097
5	65.403666	−0.422358	0.000830	−0.00000042
6	66.309376	−0.453936	0.001039	−0.00000078
7	63.836877	−0.373475	0.000483	+0.00000028
8	64.598544	−0.411766	0.000785	−0.00000035
9	67.184785	−0.471673	0.001142	−0.00000097
10	66.624937	−0.447602	0.000969	−0.00000064

Quench curve repeatability

A set of quenched samples containing ^{3}H were measured a total of ten times and the best fit cubic equation was derived for each measurement of the set. Table 15 lists the coefficients for the equation of efficiency vs. H# according to:

$$\text{Eff. } (\%) = A + B\ (H\#) + C\,(H\#)^2 + D\,(H\#)^3$$

There is some difference between the values of the coefficients, but calculation of the counting efficiencies at the same H# values for each of the 10 equations gives, basically, the same efficiencies. Table 16 lists the ten calculated efficiencies with the average efficiency, the maximum spread of % efficiency values and the % error due to the measured spread. The spread in efficiency calculated from these 10 quench curve equations is less than the quoted $\pm 1\%$ spread in counting efficiency. It is not considered accurate to calculate the efficiency based upon an H# value outside the range of H# values of the quench set. The limits of H# values for these data were the lowest H# of 26 and the highest H# of 300.

Table 16
Calculated ^3H counting efficiencies at specific H# values using each of the 10 equations given in Table 15

Eq.	Efficiency at H# equal to						
	30	50	100	150	200	250	300
1	54.39	46.75	30.78	18.88	10.53	5.18	2.29
2	53.04	46.22	31.32	19.52	10.81	5.19	2.75
3	53.50	46.13	30.63	18.99	10.71	5.33	2.34
4	53.17	45.71	30.31	18.95	10.90	5.43	1.82
5	53.47	46.31	31.04	19.31	10.77	5.13	2.05
6	53.61	46.11	30.53	18.97	10.84	5.58	2.57
7	53.08	46.42	31.60	19.64	10.70	5.04	2.83
8	52.95	45.94	30.92	19.32	10.85	5.25	2.27
9	54.03	46.34	30.46	18.86	10.77	5.48	2.27
10	54.04	46.58	30.89	19.12	10.74	5.28	2.27
Average:	53.53	46.25	30.85	19.16	10.76	5.29	2.35
Spread total	1.44	1.03	1.29	0.78	0.37	0.54	1.01
± %	0.72	0.52	0.65	0.39	0.19	0.27	0.51

Efficiency calculation repeatability

Using a single quench curve equation:

$$\text{Eff. } (\%) = 66.624937 - 0.447602\,(\text{H\#}) + 0.000969\,(\text{H\#})^2 - 0.00000064\,(\text{H\#})^3$$

a set of quenched samples, each with the same amount of ^3H, was counted 10 times. The H# value was used to calculate the counting efficiency of each sample of the set based upon the above equation. The sample dpm was calculated from the measured cpm (background corrected) and calculated counting efficiency:

$$\text{dpm} = \frac{(\text{measured cpm} - \text{bkg}) \times 100}{\text{Eff. } (\%)}$$

A constant background of 27.0 cpm was used for all H# values. Table 17 lists data obtained from the actual measurements.

The ratio of the calculated dpm to the known dpm was obtained for each of the 10 determinations of each sample of the set. Fig. 22 shows a plot of the rela-

Table 17
Calculated ^{3}H counting efficiencies based on single quench curve for actual repeated (10 times) measurement of H# values

Sample, No.	H# spread	Average H#	Average Eff., %	Spread Eff.,[a] %	Average DPM ratio[b]
1	27– 28	27.4	55.04	0.39	0.971
2	50– 54	52.6	45.89	1.41	1.002
3	85– 89	86.7	34.60	1.18	0.988
4	135–140	137.6	21.75	1.09	0.972
5	151–156	154.0	18.45	0.97	0.974
6	183–189	187.8	12.79	0.92	1.013
7	217–224	219.6	8.21	0.79	1.062
8	235–241	238.3	6.39	0.57	0.992
9	260–266	263.6	4.32	0.42	0.940
10	287–297	293.8	2.66	0.45	0.985

[a]Maximum calculated eff. (%) minus minimum calculated eff. (%).
[b]Average calculated dpm ÷ real dpm.

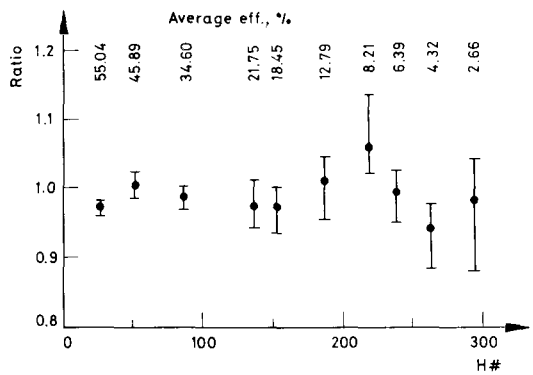

Fig. 22. Ratio of calculated DPM to real DPM as function of H# value as presented in Table 17

tive dpm ratio at each average H# value for the 10 measurements. The average of the relative ratio is indicated by an "X" while the bar indicates the spread of relative dpm ratios obtained within the set of 10 measurements.

Repeatability for ^{14}C efficiency

A set of ^{14}C containing standards was counted and the H# values measured to obtain the quench curve shown in Fig. 23. The best fit equation for this quench

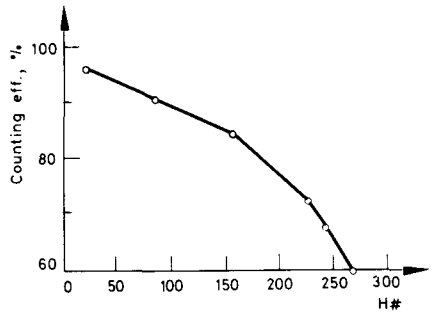

Fig. 23. Counting efficiency of ^{14}C vs. H# value for set of samples of different quench level

curve was calculated as:

$$\text{Eff. } (\%) = 97.975905 - 0.99460\,(\text{H\#}) + 0.000421\,(\text{H\#})^2 - 0.00000216\,(\text{H\#})^3$$

Using this quench curve equation, this set of ^{14}C samples was counted nine more times. The measured H# values were used to calculate the counting efficiencies and the counting efficiency was used to calculate the dpm values of the samples. The results are listed in Table 18 as Test No. 1.

The set was again counted and a second quench curve calculated. Using this new quench curve the sample set was again counted nine more times. The measured H# values were used to calculate the counting efficiencies and dpm values of the samples. These results are listed in Table 18 as Test No. 2. The results are within experimental error of those obtained in Test No. 1.

Comparison with ESCR and SCR

Fig. 24 shows the plot of ^{3}H counting efficiency vs. H# and ESCR values obtained with the same set of samples. It is noted that the ESCR value is zero at ^{3}H counting efficiency of 10% and remains zero for any lower ^{3}H counting efficiency. This data represents only one choice of External Standard counting channels.

Fig. 25 shows the plot of ^{3}H counting efficiencies vs. H# and SCR value obtained with the same set of samples. To cover the same range of quench the SCR window settings were selected to give a ratio of 0.815 for an unquenched sample. To obtain the same statistical accuracy of the ratio for the most quenched sample (SCR = 0.248) the sample had to be counted six times longer than the unquenched sample. Again this data represents only one choice of Sample Channels ratio counting channels.

Table 18
Data showing calculated ^{14}C counting efficiencies for repeated measurement of samples of different quench as measured by the H# value based upon two different quench curves: test No. 1 and test No. 2

Sample, No.	H# Spread	Average H#	Average Eff., %	Spread Eff., %	Average dpm ratio
Test No. 1					
1	22– 25	23.4	95.67	0.25	1.000
2	82– 85	83.9	91.14	0.22	1.005
3	158–164	159.7	83.88	0.79	0.995
4	219–226	221.4	73.03	1.63	1.006
5	239–243	241.3	68.04	1.09	1.001
6	267–272	269.5	59.39	1.71	1.001
Test No. 2					
1	22– 25	23.4	95.88	0.31	0.998
2	83– 85	83.1	90.90	0.14	1.009
3	158–164	159.9	84.08	0.50	0.992
4	220–226	222.6	73.10	0.43	1.003
5	237–244	240.7	68.40	1.98	0.991
6	269–277	273.2	57.72	3.02	1.028

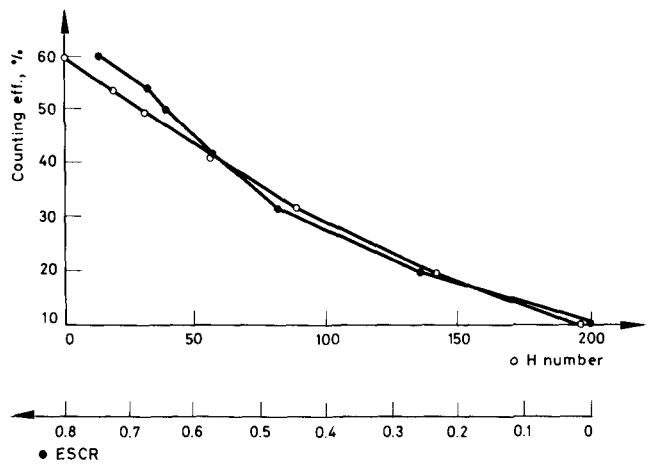

Fig. 24. Comparison of ^{3}H counting efficiency plots vs. ESCR and H# values

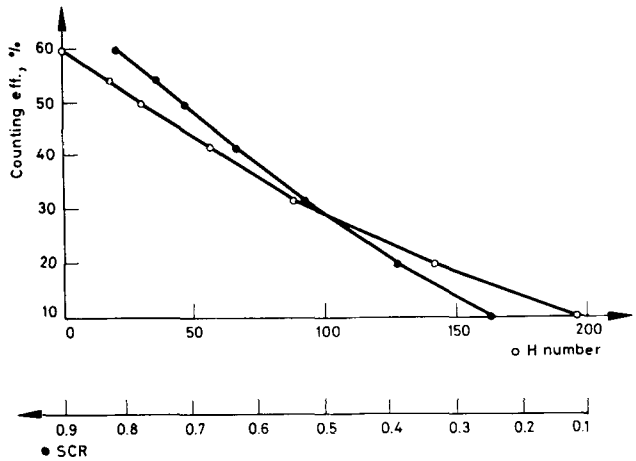

Fig. 25. Comparison of ^{3}H counting efficiency plots vs. SCR and H# values

Summary

The concept of the H# has been shown to be theoretically valid. Based upon this proof, the features of the H# concept as embodied in the Beckman LS-8000 Series Liquid Scintillation Systems have been demonstrated. It has been shown that the H# is unique, provides a method of instrument calibration and provides wide dynamic quench range measurements. Further, it has been demonstrated that the H# concept provides a universal quench parameter.

The H# concept provides a statistically repeatable measure of the quench level of any sample. Counting efficiency vs. H# plots are repeatable within the statistical limits of ±1% counting efficiency. The H# concept has made possible a very accurate method of automatic quench compensation (AQC).

The H# concept has introduced a new method of measuring sample quench level and will lead to accurate corrections of sample cpm to the actual dpm.

References

1. D. L. HORROCKS, Nucl. Instr. Meth., 30 (1964) 157.
2. D. L. HORROCKS, Nucl. Instr. Meth., 117 (1974) 589.